

# Performance of consolidants in marble and sandstone from Tuscany: a comparison

Andrea Aquino<sup>1</sup>, Marco Lezzerini<sup>1</sup>

<sup>1</sup>*Dipartimento di Scienze della Terra, Università di Pisa, Via Santa Maria 53 – 56126 Pisa, Italy,  
[andrea.aquino@phd.unipi.it](mailto:andrea.aquino@phd.unipi.it), [marco.lezzerini@unipi.it](mailto:marco.lezzerini@unipi.it)*

**Abstract** – The main goal of this preliminary study is to compare the effects of different consolidating materials on some marble and sandstone samples from Tuscany. The collected samples are divided into two groups, one of which underwent artificial weathering. A comparison on the physical properties before and after the application of the consolidating materials is given.



Figure 1. View of M. Altissimo marble quarry. Apuan Alps, Italy.

## I. INTRODUCTION

Most historical buildings, pavements and other ornamental features found in Tuscany are made of different varieties of local stones. Among these stones we find sandstone and marble, widely used in Tuscany as building and ornamental materials. Due to the nature of this lithotypes all such aforementioned structures have undergone and are still undergoing strong weathering phenomena causing them to decay and suffer a loss of the detailing found in the original ornamental features [1-4]. The main goal of this work is to compare the effectiveness of different surface treatments of various consolidants on multiple samples [5-7]. This study analyses marble and sandstone samples at different stage of weathering. Artificial aging processes, both in climatic chamber and in solar box, were carried out to simulate real degradation processes in terms of photo-thermal effects and physical-chemical damage. The stone samples used for this work come from quarries around Tuscany.



Figure 2. San Giuliano Terme marble quarry, Italy.



Figure 3. Macigno sandstone in the Greve in Chianti quarry, Italy.

## II. MATERIALS AND METHODS

The experiment has been conducted on 20 specimens of each lithotype: marble and sandstone. Each sample is a block of 8x3x3 cm<sup>3</sup>. Ten samples for each lithotype underwent artificial weathering cycles (insolation, rain and frost/ thaw). Up to ten cycles have been carried on.

We carried out the following analyses on the non-weathered specimens:

- chemical analysis through X-ray fluorescence for the determination of major and minor compounds (Na<sub>2</sub>O, MgO, Al<sub>2</sub>O<sub>3</sub>, SiO<sub>2</sub>, P<sub>2</sub>O<sub>5</sub>, K<sub>2</sub>O, CaO, TiO<sub>2</sub>, MnO, Fe<sub>2</sub>O<sub>3</sub>). The measurement uncertainty results between 4-7% by weight for concentrations <1%, between 2-4% for concentrations between 1 and 10% and around 1% for concentrations > 10% [9, 10].
- Volatile compounds content (mainly H<sub>2</sub>O<sup>+</sup> and CO<sub>2</sub>) determined by calcination (105-950°C) using a simultaneous TG-DSC thermo-microbalance Netzsch STA 449 C Jupiter according to the following operative conditions: ~25 mg fine grinded sample dust; thermal rate 10°C per minute; nitrogen flux 30 ml/min.
- CO<sub>2</sub> content measured following the gasometric method [11].
- mineralogical analysis through X ray diffractometry (XRD) (D2 Phaser by Bruker with Cu anticathode and filter NiDetector 1D Lynxeye; Diffrac.suite XRD software for acquisition and Diffrac.suite Eva software for interpretation of the data)  $\lambda = 1.5406 \text{ \AA}$ , angle range 4-66°2 $\theta$  ;

We then applied two different consolidating materials on both the weathered and non-weathered samples [12-13]:

- nano-silica in colloidal aqueous solution. SiO<sub>2</sub>

30 wt.% (10-20nm);

- calcium hydroxide nanoparticles (200nm) in isopropyl alcohol, Ca(OH)<sub>2</sub> 0,5 wt.%.



Figure 4. Apuan Alps marble as observed in thin section by optical microscope. The average grain size of the calcite crystals is about 200 microns. Upper picture parallel Nicols, lower picture crossed Nicols.

To check the variations occurred and to compare them with the non-weathered samples and the non-weathered samples after the treatment with consolidating materials, the following measurements have been carried on both non-weathered and weathered specimens:

- petrographic analyses: transmitted light microscopic observation (Zeiss AXIO Scope.A1 microscope); and scan electron microscopy using FEI Quanta 450 ESEM FEG at the *Centro Interdipartimentale di Scienza ed Ingegneria dei Materiali* of University of Pisa;
- physical properties of the stones like real ( $\rho_r$ ) and apparent ( $\rho_a$ ) density, water absorption coefficient by capillarity, water absorption at atmospheric pressure, total and open porosity have been determined following EN standards [14-15-16];
- real density ( $\rho_r$ ) has been determined using a gas pycnometer (ultra-pycnometer 1000 by

Quantachrome Corporation) on 10g dried powder;

- apparent density has been determined by ratio between dry weight and volume of each sample. The specimens were placed in a stove at 60° C until the dry weight was reached, (i.e. when the difference between two successive weighing at an interval of 24 h is not greater than 0.1 % of the mass of the specimen) [17]. Then the specimens were immersed in distilled water under vacuum for 24 hours and subsequently 24 hours more without vacuum;
- water absorption coefficient by capillarity has been determined on the same samples used for apparent density determination following [15]. Measurements taken after 1, 3, 5, 15, 30 minutes, 1 h;
- Determination of water absorption at atmospheric pressure has been carried out on the same samples. The total porosity has been calculated according to (1)

$$P \text{ (vol. \%)} = 100 \cdot (1 - \rho_a / \rho_r) \quad (1)$$

### III. RESULTS AND DISCUSSION

The analysed sandstone samples come from Matraia and have been classified as arenitic arkose [18]. Quartz, plagioclase and k-feldspar constitute almost the 75% of the stone, while the remaining 25% is mainly made by matrix, phyllosilicates, calcite and lithic fragments. The sandstone samples present the following physical properties (average): real density ( $\rho_r$ ) of 2,713 g/cm<sup>3</sup>; apparent density ( $\rho_a$ ) 2,683 g/cm<sup>3</sup>; water absorption coefficient 0,363 wt.%; total porosity 1,107 Vol.% [18].

Table 1. Average chemical composition of two marble samples (FS and P2) determined by XRF analysis: the major elements are expressed in oxides wt.%.

Sample	L.O.I.	MgO	Al <sub>2</sub> O <sub>3</sub>	SiO <sub>2</sub>	K <sub>2</sub> O	CaO	Fe <sub>2</sub> O <sub>3</sub>	Others <1%
FS	43,81	0,63	0,06	0,25	0,01	54,96	0,01	0,28
P2	43,92	0,80	0,07	0,15	0,01	54,84	0,02	0,20

L.O.I. = Loss on ignition; Fe<sub>2</sub>O<sub>3</sub> = Total Iron as Fe<sub>2</sub>O<sub>3</sub>.

For the purpose of this preliminary work, we selected two marble samples, FS and P2 for the sake of comparison. Sample FS, is a marble characterised by inequigranular granoblastic texture, mainly made by calcite. Grain size of calcite crystals has a mean value of 275 µm and a maximum value of 860 µm. Albite, quartz and pyrite were observed as accessory phases (Table 2). Sample P2, is a marble with inequigranular granoblastic/xenoblastic texture, mainly made by calcite. Grain size of calcite crystals has a mean value of 225 µm and a maximum value of 640 µm. Occasional veins filled with quartz and pyrite are found (Table 2).

Overall, the studied marble samples are <98% pure CaCO<sub>3</sub> where the insoluble residue is made by albite,

quartz, pyrite and phyllosilicates. (Tables 1 and 2) [19].

Table 2. Mineral phases presence in marble samples.

Sample	Albite	Quartz	Dolomite	Pyrite	Phyllosilicate
FS	x	x		x*	x
P2		x	x	x	x

x= presence; \*= petrographic analyses

The physical properties for the marble samples are reported in table 3.

Table 3. Main physical properties. G = Real density (g/m<sup>3</sup>);  $\gamma_d$  = apparent density (g/m<sup>3</sup>); CA =water absorption by capillarity coefficient (%); CI<sub>P</sub> = imbibition coefficient referred to sample real volume (%); CI<sub>V</sub> = imbibition coefficient referred to apparent volume of the sample (%); P = porosity (Vol. %); IS = Saturation index (%).

Sample	G	$\gamma_d$		CA		CI <sub>P</sub>	
		M	$\sigma$	M	$\sigma$	M	$\sigma$
FS	2.720	2.705	0,001	0,086	0,023	0,12	0,01
P2	2.717	2.709	<0,001	0,032	0,008	0,08	<0,01

Sample	CI <sub>V</sub>		P		IS	
	M	$\sigma$	M	$\sigma$	M	$\sigma$
FS	0,32	0,04	0,37	0,05	86	8
P2	0,23	0,01	0,25	0,02	91	4

The effects of the treatment with calcium hydroxide nanoparticles are valuable on the highly weathered marble samples (Fig. 6), while the other less weathered ones show almost no variations in the water absorption.

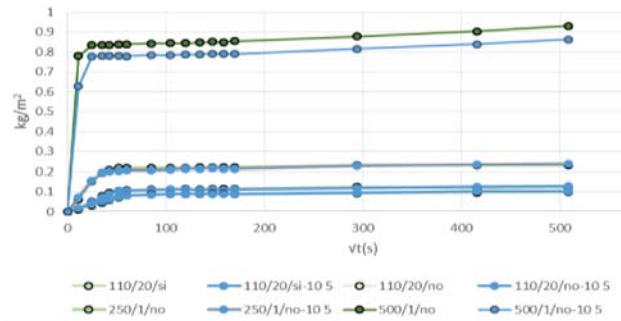


Figure 6. Diagram showing the water absorption of marble samples before (green) and after (blue) treatment with calcium hydroxide nanoparticles.

The use of nano-silica in colloidal aqueous solution instead, has shown a significant variation in the water absorption values both in non-weathered and weathered samples (Fig. 7).

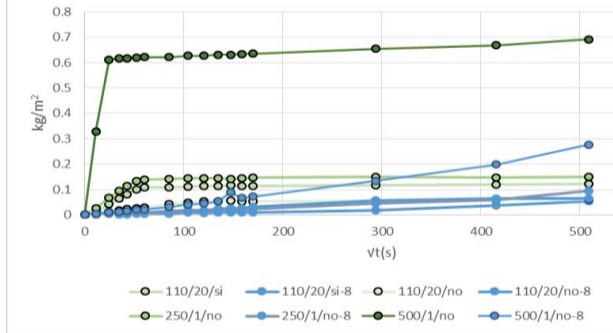


Figure 7. Diagram showing the water absorption of marble samples before (green) and after (blue) treatment with silica nanoparticles.

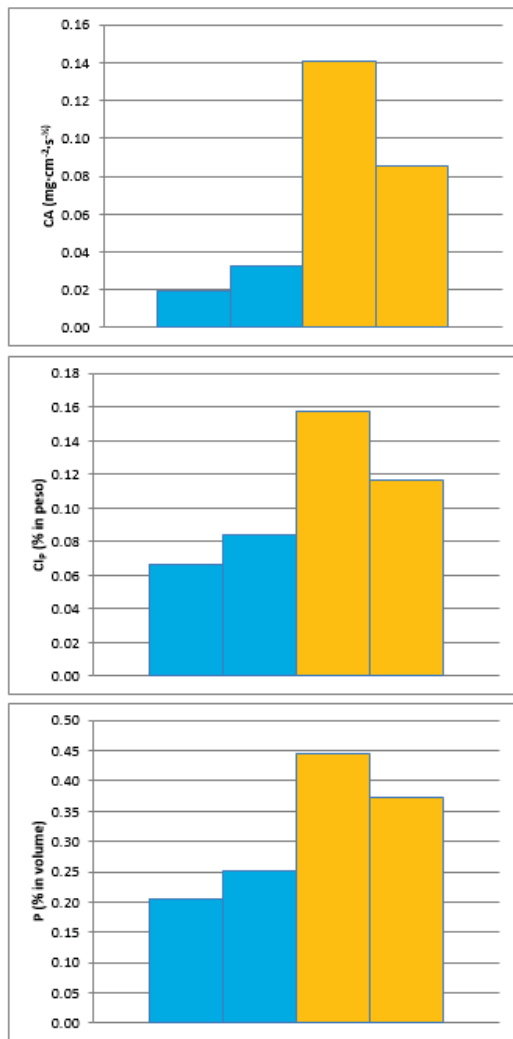


Figure 8. Diagrams showing the main differences of CA, Cl<sub>2</sub> and P of samples P2 (Blue) and FS (Yellow)

The different behaviour of these two consolidating materials on marbles are due to the size of the nanoparticles used. Indeed, the silica particles are ten times smaller than the calcium hydroxide ones, whose size is comparable to the one of the calcite crystals themselves.

Studies on the effects of the treatments on the sandstone samples are still ongoing.

#### IV. CONCLUSIONS

Thanks to its nanoparticle size, both products can be used as consolidating materials. Better performances are for more weathered and deteriorated samples. Calcium hydroxide nanoparticles (200nm) require multiple treatments to guarantee results comparable to the one of nanosilica (10-20nm).

#### V. ACKNOWLEDGMENT

We want to thank Alessio Ascione for his help in getting some of the data presented in this work.

#### REFERENCES

- [1] Amoroso, G.G., Fassina, V. (1983) Stone Decay and Conservation.
- [2] Garzonio, C.A., Cantisani, E. Mechanical decay and degradation of marble slabs. (2006) Proceedings of the International Symposium of the International Society for Rock Mechanics, Eurock 2006 - Eurock 006 Multiphysics Coupling and Long-Term Behaviour in Rock Mechanics pp. 461-466.
- [3] Garzonio, C.A., Fratini, F., Manganeli del Fà, C., Giovannini, P., Blasi, C. Analysis of geochemical decay phenomena of marbles employed in historical monuments in Tuscany (1995) Proceeding of MJFR, 2nd International Conference, pp. 259-263.
- [4] Rodríguez-Gordillo, J., Sáez-Pérez, M.P. Effects of thermal changes on Macael marble: Experimental study (2006) Construction and Building Materials, 20 (6), pp. 355-365.
- [5] D'Amato, R., Caneve, L., Giancristofaro, C., Persia, F., Piloni, L., Rinaldi, A. Development of nanocomposites for conservation of artistic stones (2014) Proceedings of the Institution of Mechanical Engineers, Part N: Journal of Nanoengineering and Nanosystems, 228 (1), pp. 19-26.
- [6] Kim, E.K., Won, J., Do, J.-y., Kim, S.D., Kang, Y.S. Effects of silica nanoparticle and GPTMS addition on TEOS-based stone consolidants (2009) Journal of Cultural Heritage, 10 (2), pp. 214-221.
- [7] Mosquera, M.J., De Los Santos, D.M., Montes, A., Valdez-Castro, L. New nanomaterials for consolidating stone (2008) Langmuir, 24 (6), pp. 2772-2778.

- [8] Franzoni, E., Sassoni, E., Scherer, G.W., Naidu, S., Artificial weathering of stone by heating.
- [9] Franzini M., Leoni L., Saitta M., 1975. Revisione di una metodologia analitica per fluorescenza-X, basata sulla correzione completa degli effetti di matrice. *Rend. Soc. It. Mineral. Petrog.*, 31: 365-378.
- [10] Lezzerini M., Tamponi M., Bertoli M., 2014. Calibration of XRF data on silicate rocks using chemicals as in-house standards. *Atti Soc. Tosc. Sci. Nat., Mem., Serie A*, 121: 65-70.
- [11] Leone G, Leoni L, Sartori F., 1988. Revisione di un metodo gasometrico per la determinazione di calcite e dolomite. *Atti Soc. Tosc. Sci. Nat., Mem., Serie A*, 95: 7-20.
- [12] Cámara, L., Estívariz, E., Fernández, B., García, P., Koroso, I., Narbona, B., Tamayo, S., Lazzeri, A., Vicini, I., Castelvetro, V., Toniolo, L., Lezzerini, M., Weber, J., Mascha, E., Ban, M., Rohatsch, A., Drewello, R., 2018. Santa maría de vitoria: Primeros pasos en la conservación de sus muros mediante nanomateriales. proyecto NANO-cathedral. REHABEND, (221479), pp. 1557-1565.
- [13] Raneri, S., Giannoncelli, A., Mascha, E., Toniolo, L., Roveri, M., Lazzeri, A., Coltelli, M.B., Panariello, L., Lezzerini, M., Weber, J., 2019. Inspecting adhesion and cohesion of protectives and consolidants in sandstones of architectural heritage by X-ray microscopy methods *Materials Characterization*, 156, art. no. 109853.
- [14] EN 1936:2007 - Natural stone test methods - Determination of real density and apparent density, and of total and open porosity.
- [15] EN 1925:1999 - Natural stone test methods - Determination of water absorption coefficient by capillarity.
- [16] EN 13755:2008 - Natural stone test methods - Determination of water absorption at atmospheric pressure.
- [17] Franzini M., Lezzerini M., 2003. A mercury-displacement method for stone bulk-density EN 14581:2005 - Natural stone test methods - Determination of linear thermal expansion coefficient.
- [18] Lezzerini, M., Franzini, M., Di Battistini, G., Zucchi, D., 2008. The «macigno» sandstone from Matraia and Pian di Lanzola quarries (north-western Tuscany, Italy ). A comparison of physical and mechanical properties. *Atti della Società Toscana di Scienze Naturali, Memorie Serie A*, 113, pp. 71-79.
- [19] Lezzerini, M., Di Battistini, G., Zucchi, D., Miriello, D., 2012. Provenance and compositional analysis of marbles from the medieval Abbey of San Caprasio, Aulla (Tuscany, Italy). *Applied Physics A: Materials Science and Processing*, 108 (2), pp. 475-485.